Title

Adrenic Acid-Derived Epoxy Fatty Acids Are Naturally Occurring Lipids and Their Methyl Ester Prodrug Reduces Endoplasmic Reticulum Stress and Inflammatory Pain

Journal

ACS Omega, 6(10)

ISSN

2470-1343

Authors

Singh, Nalin

Barnych, Bogdan

Wagner, Karen M

et al.

Publication Date

2021-03-16

DOI

10.1021/acsomega.1c00241

Peer reviewed

ACS OMEGA

http://pubs.acs.org/journal/acsodf

Article

Adrenic Acid-Derived Epoxy Fatty Acids Are Naturally Occurring Lipids and Their Methyl Ester Prodrug Reduces Endoplasmic Reticulum Stress and Inflammatory Pain

Nalin Singh, Bogdan Barnych, Karen M. Wagner, Debin Wan, Christophe Morisseau, and Bruce D. Hammock*

Cite This: *ACS Omega* 2021, 6, 7165−7174

Read Online

ACCESS | Metrics & More | Article Recommendations | Supporting Information

ABSTRACT: Adrenic acid (AdA, 22:4) is an ω-6 polyunsaturated fatty acid (PUFA), derived from arachidonic acid. Like other PUFAs, it is metabolized by cytochrome P450s to a group of epoxy fatty acids (EpFAs), epoxydocosatrienoic acids (EDTs). EpFAs are lipid mediators with various beneficial bioactivities, including exertion of analgesia and reduction of endoplasmic reticulum (ER) stress, that are degraded to dihydroxy fatty acids by the soluble epoxide hydrolase (sEH). However, the biological characteristics and activities of EDTs are relatively unexplored, and, alongside dihydroxydocosatrienoic acids (DHDTs), they had not been detected *in vivo*. Herein, EDT and DHDT regioisomers were synthesized, purified, and used as standards for analysis with a selective and quantitative high-performance liquid chromatography-tandem mass spectrometry (HPLC-MS/MS) method. Biological verification in AdA-rich tissues suggests that basal metabolite levels are highest in the liver, with 16,17-EDT concentrations consistently being the greatest across the analyzed tissues. Enzyme hydrolysis assessment revealed that EDTs are sEH substrates, with greatest relative rate preference for the 13,14-EDT regioisomer. Pretreatment with an EDT methyl ester regioisomer mixture significantly reduced the onset of tunicamycin-stimulated ER stress in human embryonic kidney cells. Finally, administration of the regioisomeric mixture effectively alleviated carrageenan-induced inflammatory pain in rats. This study indicates that EDTs and DHDTs are naturally occurring lipids, and EDTs could be another therapeutically relevant group of EpFAs.

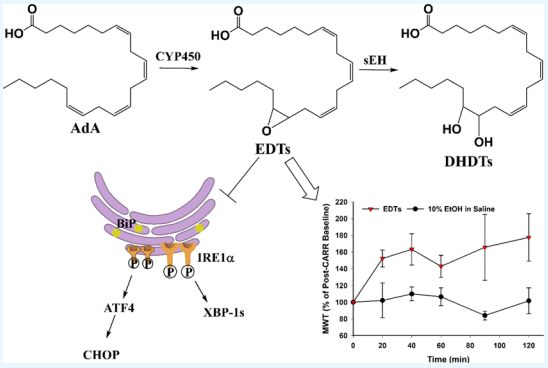

INTRODUCTION

A subset of cytochrome P450s (CYPs) mediate oxidation of polyunsaturated fatty acids (PUFAs), generating monoepoxide metabolites known as epoxy fatty acids (EpFAs). EpFAs are signaling molecules that play a role in various pathologies and exert primarily anti-inflammatory, antihypertensive, analgesic, antiapoptotic, and antiendoplasmic reticulum (ER) stress effects.[1−5] Epoxyeicosatrienoic acids (EETs), derived from the ω-6 PUFA arachidonic acid (ARA, 20:4), are the most widely studied group of EpFAs. Other relevant EpFAs include ω-3 PUFAs docosahexaenoic acid (DHA, 22:6) and eicosapentaenoic acid (EPA, 20:5)-derived epoxydocosapentaenoic acids (EDPs) and epoxyeicosatetraenoic acids (EEQs), respectively. EpFAs are rapidly degraded *in vivo* to less active dihydroxy fatty acids (DHFAs) chiefly by the soluble epoxide hydrolase (sEH). sEH inhibition is a common therapeutic approach that stabilizes EpFA levels *in vivo*, enhancing their bioavailability and biological functions.

All-*cis*-7,10,13,16-docosatetraenoic acid (DTA, 22:4), more commonly known as adrenic acid (AdA), is another ω-6 PUFA. It is formed *via* 2-carbon elongation of ARA at the carboxylic end or elongation and desaturation of linoleic acid (LA, 18:2).[6−8] It is present in the adrenal gland, liver, kidney, brain, and vasculature.[8−11] Exogenous administration of AdA in *ex vivo* arterial models induced CYP-mediated formation of a group of EpFAs, epoxydocosatrienoic acids (EDTs, also known as DH-EETs).[12,13] Diol metabolites, dihydroxydocosatrienoic acids (DHDTs, also known as DH-DHETs), were also detected,[13] presumably formed by downstream sEH hydrolysis.

EDTs were found to be endothelium-derived hyperpolarizing factors with strong vasorelaxant effects.[12,13] Another study demonstrated the ability of EDTs to dilate coronary microvessels.[14] The mode of action was consistent with the established vasodilatory mechanism of EETs.[15−17] Despite this biological activity and structural relevance, the role of EDTs is not well studied and the occurrence of EDTs and

Received: January 13, 2021
Accepted: February 18, 2021
Published: March 2, 2021

https://dx.doi.org/10.1021/acsomega.1c00241
ACS Omega 2021, 6, 7165−7174

DHDTs has not been previously reported *in vivo*. The lack of a sufficiently sensitive and reliable analytical method is a key limiting factor, as is the absence of commercially available EDT and DHDT standards.

Hence, to illuminate the physiological characteristics and bioactivities of a relatively unexplored metabolite pairing, the epoxy and dihydroxy metabolites of AdA were synthesized and purified. A sensitive, selective, and reliable high-performance liquid chromatography-tandem mass spectrometry (HPLC-MS/MS) method was developed and used to quantify basal metabolite concentrations and distributions in AdA-rich tissues. The method was then applied to an enzyme kinetics study to assess the rate of sEH-mediated hydrolysis of EDT regioisomers. Finally, the therapeutic action of an EDT methyl ester regioisomer mixture was investigated (1) *in vitro* against tunicamycin-triggered ER stress in human embryonic kidney (HEK293) cells (2) *in vivo* against carrageenan-induced inflammatory pain in rats.

RESULTS AND DISCUSSION

Multiple Reaction Monitoring (MRM) Transitions, Retention Times, and Method Validation. Since the m/z of each parent epoxide or diol ion was the same, the developed HPLC-MS/MS analytical method emphasized both unique, quantitative ion transitions and chromatographic separation to effectively distinguish regioisomers. Most molecular fragmentation occurred near the epoxide or diol functional groups. Since the position of those groups varies depending on the location of the double bond, a specific fragmentation pattern followed, yielding distinctive daughter ions for every regioisomer (Table 1). With regards to chromatography, the

Table 1. Optimized MRM Transitions, Retention Times, Method Limits of Detection and Quantitation, and Linear Ranges for EDTs and DHDTs

analyte	Q1 (Da)	Q3 (Da)	t_R (min)	LOD (pM)	LOQ (pM)	linear range (nM)
16,17-DHDT	365.5	235.0	6.44	50	100	0.125−200
13,14-DHDT	365.5	195.1	6.58	50	100	0.125−200
10,11-DHDT	365.5	154.9	6.67	10	50	0.125−200
7,8-DHDT	365.5	96.9	6.78	100	500	0.625−200
16,17-EDT	347.2	246.9	8.25	5	10	0.0125−200
13,14-EDT	347.2	194.9	8.44	5	10	0.0125−200
10,11-EDT	347.2	182.9	8.50	10	50	0.125−200
7,8-EDT	347.2	134.9	8.71	500	1000	1.25−200

DHDTs expectedly eluted much earlier than the EDTs from the reverse phase LC column (Table 1) since they are considerably more polar.[13] Furthermore, within each metabolite group, regioisomers with groups at the terminal double bond (*i.e.*, 16,17) eluted first (Table 1) as the distance between the epoxide or diol moiety and the carboxylic end of the acid directly correlates with polarity.[13] The large linear, dynamic range and low limits of detection and quantitation (Table 1) indicate that the method can be applied in making quantitative assessments over a varying range of analyte concentrations, including at very low levels. Both intraday and interday precision and accuracy were consistently >84% (Table S1, Supporting Information), signifying reliable and reproducible quantitation of samples. Analytical recovery of the method at low, moderate, and high compound concentrations was >85% (Figure S1, Supporting Information), demonstrating efficient and consistent biological sample preparation and analyte extraction.

Occurrence and Distribution of Basal EDT and DHDT Levels in Rat Tissues. Previously, CYP-mediated generation of EDTs was demonstrated through exogenous administration of adrenic acid in *ex vivo* arterial systems.[12,13] However, their occurrence *in vivo* was unclear. Hence, basal EDT and DHDT concentrations were quantified in tissues reported to have abundant levels of AdA. Most of the metabolites were detected in rat liver, kidney, and brain samples, and levels were found to be highest in the liver (Table 2). This finding can potentially

Table 2. Concentrations of EDTs and DHDTs in AdA-Rich Rat Tissues[a]

absolute concentrations (pg/g of tissue)				relative concentrations (% of analogous ARA metabolite)			
	liver	brain	kidney		liver	brain	kidney
7,8-EDT	N/D	N/D	N/D	7,8-EDT/5,6-EET	N/D	N/D	N/D
10,11-EDT	40.6	N/D	N/D	10,11-EDT/8,9-EET	7.03	N/D	N/D
13,14-EDT	47.0	18.8	8.31	13,14-EDT/11,12-EET	4.73	2.67	0.55
16,17-EDT	186	41.6	45.5	16,17-EDT/14,15-EET	31.7	8.50	3.25
7,8-DHDT	N/D	N/D	N/D	7,8-DHDT/5,6-DHET	N/D	N/D	N/D
10,11-DHDT	N/D	N/D	20.9	10,11-DHDT/8,9-DHET	N/D	N/D	0.63
13,14-DHDT	107	N/D	16.8	13,14-DHDT/11,12-DHET	0.97	N/D	0.94
16,17-DHDT	115	N/D	24.3	16,17-DHDT/14,15-DHET	0.66	N/D	0.32

[a]N/D indicates <LOQ.

be attributed to greater hepatic CYP and sEH expression,[18,19] relative to other organs, resulting in more localized biosynthesis. DHDTs were below the limit of quantitation (LOQ) in the brain (Table 2) which may be due to the greater polarity of DHFAs, which is considered to facilitate rapid transport to and accumulation in the cerebrospinal fluid, as has been observed for dihydroxyeicosatrienoic acids (DHETs).[20] The 16,17-EDT regioisomer was consistently present at the highest concentrations across all three tissues, particularly in the liver (Table 2). This indicates that the CYP-facilitated epoxidation of AdA likely occurs preferably at the terminal olefin. The phenomenon would be consistent with the catalytic preference CYP monooxygenases have for the terminal double bond in several PUFAs and endocannabinoids.[21,22] 13,14-EDT and 16,17-EDT were also detected in rat plasma, at concentrations of 0.112 and 0.369 nM, respectively. In general, relative levels of EDTs (0.6−9%) and DHDTs (0.3−1%) in tissues were considerably lower than those of structurally analogous EETs and DHETs (defined as the metabolite with corresponding functional group located at identical olefin position, e.g., terminal epoxides 16,17-EDT and 14,15-EET, Table 2). The finding would be in line with the lower systemic abundance of the parent AdA, relative to ARA. The notable exception was

https://dx.doi.org/10.1021/acsomega.1c00241
ACS Omega 2021, 6, 7165−7174

hepatic 16,17-EDT, which was present at nearly one-third of the concentrations of 14,15-EET.

Kinetic Parameters of EDTs for Human sEH. Previously, the formation of DHDTs has been observed following the administration of AdA in adrenal cortical arteries.[13] sEH hydrolysis of EDTs was the suspected route of metabolism since it is the primary pathway of degradation for other EpFAs. However, this hypothesis was not tested until this study, which reveals EDTs to be sEH substrates. The ability of sEH to hydrolyze each EDT regioisomer was studied under steady-state conditions using purified, recombinant human sEH. The enzyme catalysis for all of the substrates fits the Michaelis–Menten model well (R^2 = 0.95–0.99, Figure 1), and variability

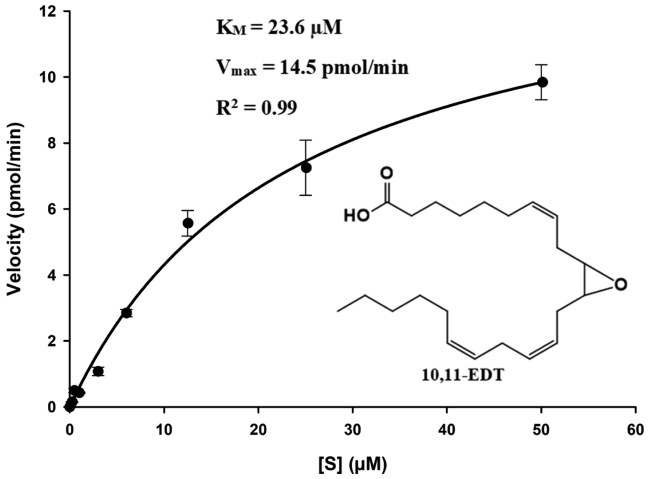

Figure 1. Velocity *vs* [S] plot for hydrolysis of 10,11-EDT by recombinant, human sEH ([E] = 3 nM). The kinetic constants (K_M and V_{max}) were determined by nonlinear regression using the enzyme kinetic module of SigmaPlot 14.0 (Systat Software, Inc.). An R^2 of 0.99 indicates that the reaction fits the Michaelis–Menten model well.

Table 3. Kinetic Parameters for Hydrolysis of EDT Regioisomers by Recombinant Human sEH

	R^2	K_M (μM)	k_{cat} (s^{-1})	k_{cat}/K_M ($s^{-1}/\mu M^{-1}$)
7,8-EDT	0.95	30.2	0.26	0.009
10,11-EDT	0.99	23.6	0.40	0.017
13,14-EDT	0.97	6.37	0.58	0.091
16,17-EDT	0.98	23.1	0.67	0.029
8,9-EET[a]	0.97	26.0	0.56	0.022
11,12-EET[a]	0.97	2.0	0.26	0.13
14,15-EET[a]	0.95	7.0	3.0	0.43

[a]Literature values.[25]

in kinetic constants was observed (Table 3). K_M and V_{max} were acquired through nonlinear regression and k_{cat} (*i.e.*, turnover number) was obtained by dividing maximal velocity by enzyme concentration. The mechanism of sEH hydrolysis is a two-step base-catalyzed process that involves the formation of a covalent hydroxyl–alkyl–enzyme ester intermediate, followed by ester hydrolysis by water and the release of the vicinal diol.[23] Hence, the K_M value is a measurement for the substrate concentration at which velocity is half-maximal, rather than a measure of enzymatic affinity for the substrate. The k_{cat} value represents primarily the rate constant for hydrolysis of the covalent intermediate since that is the slower, rate limiting step.[24] The k_{cat}/K_M ratio is a measure of enzyme efficiency and is the most comprehensive indicator of the rate of reaction for a substrate. The ratio was greatest for 13,14-EDT (Table 3), indicating it was the best sEH substrate within the group. Accordingly, 16,17-EDT and 10,11-EDT were the next most preferred substrates, respectively, while 7,8-EDT was the worst (Table 3). The variable regioisomeric selectivity was consistent with sEH hydrolysis trends observed for other EpFAs such as EETs, EDPs, and EEQs.[25] Generally, within each EpFA group, the regioisomer with the epoxide around carbon-14 (e.g., 13,14-EDP or 14,15-EET) is degraded most rapidly[25] and the greatest relative substrate selectivity for 13,14-EDT was in line with this phenomenon. The rate of metabolism worsens or ceases as the epoxide in the molecule approaches the terminal or carboxylic ends (e.g., 19,20-EDP or 5,6-EET).[25] Expectedly, 7,8-EDT was the most slowly hydrolyzed regioisomer due to the proximity of its epoxide group to the acid function. The sEH active site is probably the key consideration in determining selectivity.[26] It includes large hydrophobic pockets on either side of the catalytic triad residues and, hence, accommodates EpFAs that possess the epoxide closer to the middle of the chain most effectively. A comparison with the kinetics of hydrolysis for EETs[25] indicates that EDTs are, in general, poorer substrates for the sEH (Table 3). While the rates of hydrolysis for 10,11-EDT and 13,14-EDT were quite similar to those of homologous EETs (*i.e.*, 8,9-EET and 11,12-EET, respectively, Table 3), the k_{cat}/K_M of 16,17-EDT was smaller than that of 14,15-EET by more than 1 order of magnitude (Table 3). This indicates 16,17-EDT is hydrolyzed significantly more slowly than its EET homologue and hence would possess greater resistance to degradation, which could be a factor that accounts for its relatively higher concentrations *in vivo* compared to other EDT/EET pairings (Table 2).

Downregulation of Tunicamycin-Triggered Endoplasmic Reticulum Stress in Human Embryonic Kidney Cells. Disruptions to endoplasmic reticulum (ER) homeostasis result in the accumulation of misfolded proteins in the ER lumen, a phenomenon known as ER stress.[27] The downstream unfolded protein response (UPR) is activated, which is adaptive during early-stage ER stress but shifts towards apoptotic signaling if the system is overwhelmed under late-stage conditions. EETs and soluble epoxide hydrolase inhibitors have demonstrated the ability to stabilize the ER stress response and, consequently, ameliorate a variety of pathologies.[28] Hence, the ability of EDTs to mediate ER stress was explored in HEK293 cells, utilizing a tunicamycin model to simulate ER stress conditions.[29] Pretreatment with EDT methyl esters improved cell viability following prolonged exposure to tunicamycin (Figure 2), in a dose-dependent manner (Figure 2B). EDTs also reduced UPR markers in cells exposed to tunicamycin, during conditions of both early- (5 h, Figure 3) and late- (16 h, Figure 4) stage ER stress. Finally, EDTs decreased the activity of a tunicamycin-activated inflammatory caspase (*i.e.*, caspase-1, Figure 4C). The magnitude of effects exerted was comparable to that of EET methyl esters pretreated cells (Figures 2A, 3, and 4). During early-stage ER stress, restoration of the master ER chaperone binding immunoglobulin protein (BiP) to basal levels (Figure 3B), diminished phosphorylated/total ratio of the UPR transducing inositol-requiring enzyme 1α (IRE1α) (Figure 3C), and abolished activation of the chaperone-transcribing spliced X-box binding protein 1 (XBP-1s) (Figure 3A) imply

https://dx.doi.org/10.1021/acsomega.1c00241
ACS Omega 2021, 6, 7165–7174

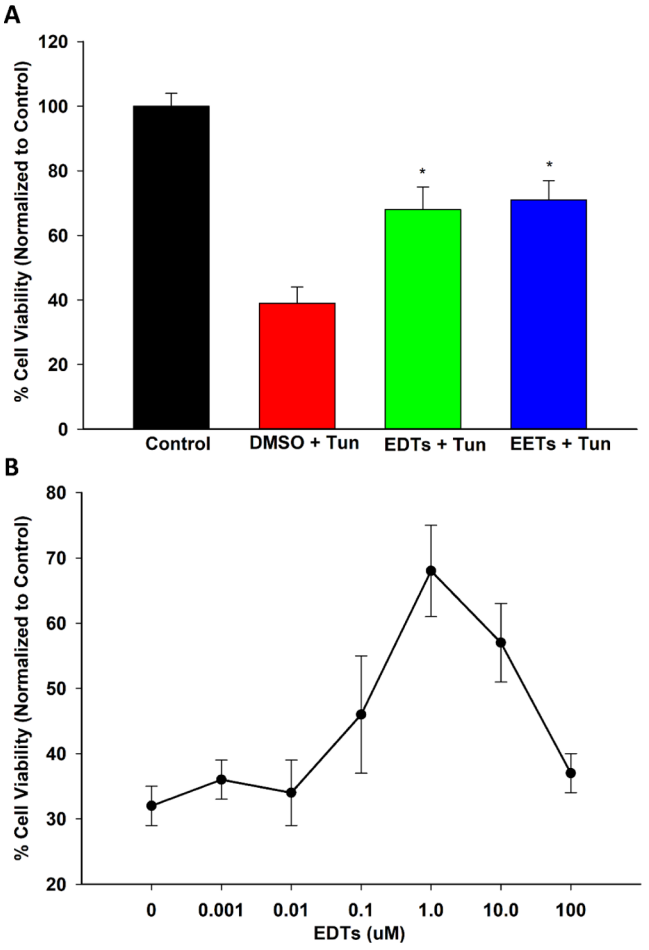

Figure 2. EDTs restore the viability of HEK293 cells exposed to tunicamycin (Tun). (A) Pretreatment with EDTs (methyl esters, regioisomeric mixture, 1 μM) or EETs significantly improved cell viability following prolonged (24 h) exposure to 4 μg/mL Tun (one-way analysis of variance, Holm−Sidak method, *$p < 0.001$ *vs* dimethyl sulfoxide (DMSO) + Tun group, $\alpha = 0.05$). (B) Dose response of the protective action of EDTs, with maximal therapeutic activity occurring at a 1 μM dose of EDT methyl esters (regioisomer mixture).

EDTs help ameliorate the misfolded protein burden on the ER and re-establish homeostatic folding capacity. The diminished levels of a transcription factor, activating transcription factor 4 (ATF4) (Figure 4B) and termination of C/EBP homologous protein (CHOP) upregulation (Figure 4A) during late-stage ER stress indicate that EDTs play a role in blocking augmentation of downstream proapoptotic pathways. ER stress has shown to induce caspase-1, an inflammasome-linked caspase implicated in apoptotic and pyroptotic cell death signaling.[30] Its activity was elevated by tunicamycin but substantially curbed by EDT pretreatment (Figure 4C), suggesting EDTs might mitigate proinflammatory responses initiated by perturbations to the ER.

Analgesia Against Carrageenan-Induced Inflammatory Pain. Regioisomeric mixtures of EETs, EDPs, and EEQs and soluble epoxide hydrolase inhibitors have been shown to effectively alleviate inflammation-mediated pain.[25,31] Hence, the potential antinociceptive activity of EDTs was also investigated, utilizing a previously described carrageenan-induced inflammatory pain model in rats.[25] Administration of carrageenan considerably reduced paw withdrawal thresholds (compared to naïve baseline), indicating the development of a severely painful state. Treatment with EDT methyl esters significantly increased paw withdrawal thresholds (Figure 5A,B), over a 2 h time course, indicating pain relief. The intensity of effect was also comparable to that of EET methyl esters-treated rats (Figure 5).

CONCLUSIONS

The inhibition of soluble epoxide hydrolase is a novel and promising therapeutic approach that could potentially tackle several unmet clinical needs, ranging from acute and chronic pain to various fibrotic, metabolic, renal, and neurodegenerative disorders.[28,31−33] The underlying bioactivity of EpFAs dictates the efficacy of sEH inhibitors (sEHI) and has primarily been attributed to the ARA-derived EETs, though more recently there is growing interest in the biological roles of epoxy metabolites of ω-3 PUFAs, namely EDPs and EEQs. Based on the results of this study, AdA-derived EDTs (Figure 6) appear to be another relevant class of EpFAs. With the synthesis of regioisomer standards and through validated HPLC-MS/MS analysis of AdA-rich tissues, this study establishes that EDTs are indeed naturally occurring lipids *in vivo*. Furthermore, the demonstrated capability of EDTs to attenuate ER stress, the signaling response that underlies several aforementioned pathologies, as well as reduce inflammatory pain strengthens the case that EDTs are pertinent lipid mediators. Finally, the finding that EDTs are metabolized by sEH (Figure 6) implies that inhibition of sEH would stabilize their levels *in vivo*. This suggests that EDTs may in part contribute to the efficacy of sEHI and hence future studies should consider the bioactivity of EDTs when the therapeutic effects of sEHI are examined in disease models.

METHODS

Reagents and General Experimental Procedures. Adrenic methyl ester was purchased from Nu-Chek Prep, Inc. (Elysian, MN). All chemicals purchased from commercial sources were used as received without further purification. Acetonitrile, methanol, ethyl acetate, and glacial acetic acid of HPLC grade or better were purchased from Fisher Scientific (Pittsburgh, PA). The internal standard, 12-(3-cyclohexyl-ureido)-dodecanoic acid (CUDA), was synthesized in-house and dissolved in methanol. Deionized water (18.1 MΩ/cm) was prepared in-house and used for mobile phase preparation and solid-phase extraction (SPE). Tunicamycin (10 mg/mL in DMSO) was purchased from Alfa Aesar (Haverhill, MA). Ac-VAD-AFC, a fluorogenic caspase-1 substrate, was purchased from Santa Cruz Biotechnology, Inc. (Dallas, TX). Primary antibodies against BiP (C50B12), IRE1α (14C10), *p*-IRE1α (Ser724), XBP-1s (D2C1F), ATF4 (D4B8), and CHOP (L63F7) were purchased from Cell Signaling Technology (Danvers, MA) or Thermo Fisher Scientific (Waltham, MA). Analytical TLC was performed on Merck TLC silica gel 60 F254 plates and spots were visualized *via* potassium permanganate staining. Flash chromatography was performed on silica gel (230−400 mesh) from Macherey Nagel. ^{1}H and ^{13}C NMR spectra were recorded on 400 MHz Bruker Avance III HD Nanobay or 800 MHz Avance III NMR spectrometers and referenced to the residual solvent peak at δ 7.28 or δ 1.94 ($CDCl_3$ or CD_3CN) and δ 77.14 ($CDCl_3$), respectively. Multiplicity is described by the abbreviations, s = singlet, t = triplet, and m = multiplet. High-resolution electrospray

https://dx.doi.org/10.1021/acsomega.1c00241
ACS Omega 2021, 6, 7165−7174

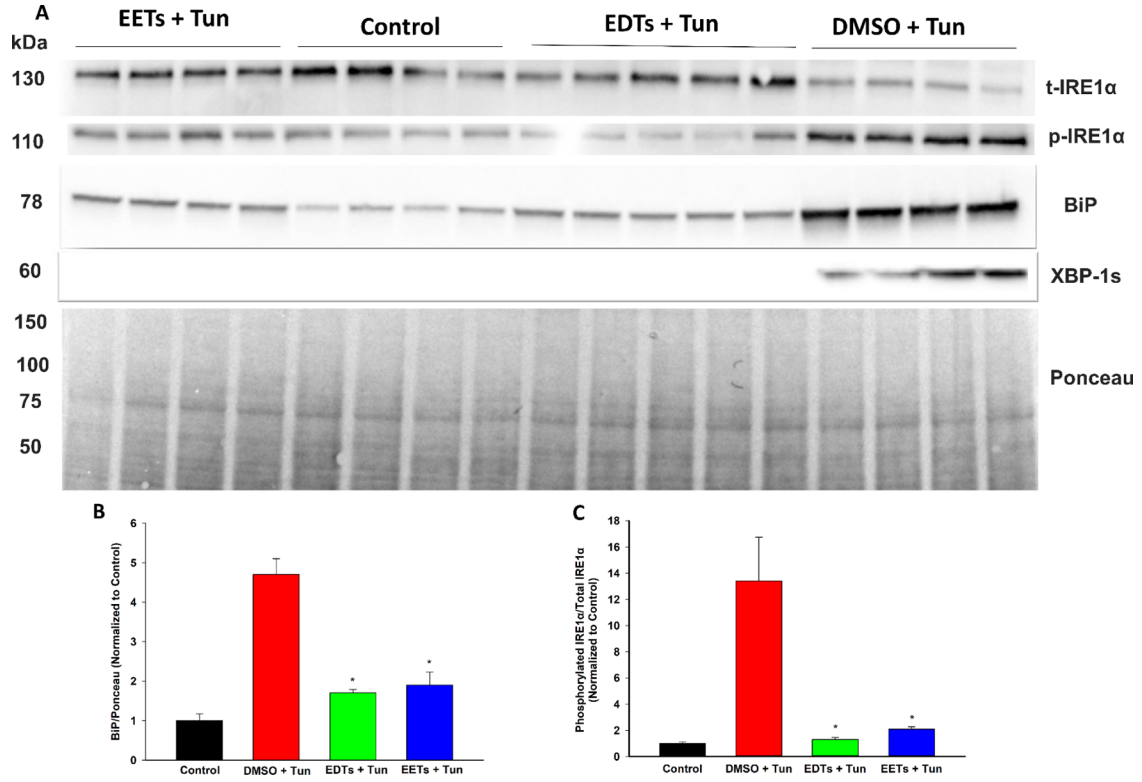

Figure 3. EDTs attenuate early-stage UPR markers in tunicamycin (Tun)-triggered ER stress in HEK293 cells. (A) Immunoblots of *t*-IRE1α, *p*-IRE1α, BiP, and XBP-1s for cells pretreated with EDTs (methyl esters, regioisomeric mixture, 1 μM), EETs, or DMSO for 1 h and exposed to 4 μg/mL Tun for 5 h. (B) EDTs (and EETs) significantly reduced BiP levels, relative to Ponceau loading control (one-way analysis of variance, Holm-−Sidak method, *p < 0.001 *vs* DMSO + Tun group, α = 0.05). (C) EDTs (and EETs) significantly reduced the ratio of phosphorylated IRE1α to total IRE1α (one-way analysis of variance, Holm−Sidak method, *p < 0.001 *vs*. DMSO + Tun group, α = 0.05).

ionization mass spectroscopy (HRESIMS) was recorded on a Thermo Q-Exactive high-field orbitrap mass spectrometer, equipped with an electrospray ionization source operating in the positive- or negative-ion mode.

Synthesis, Characterization, and Application of EDT Methyl Esters (Regioisomeric Mixture). Adrenic methyl ester (1.00 g, 2.89 mmol, 1.0 equiv) was quickly added to a vigorously stirring solution of 70% *meta*-chloroperoxybenzoic acid (143 mg, 0.578 mmol, 0.20 equiv) in dichloromethane and stirred for 90 min at room temperature. The reaction was quenched with saturated sodium carbonate (aq) and the mixture was extracted with diethyl ether (4×), dried ($MgSO_4$), and concentrated under reduced pressure. EDT methyl esters were purified by flash chromatography (ethyl acetate−hexanes 10:90). Colorless oil; ^{1}H NMR (400 MHz, $CDCl_3$) δ 5.52−5.26 (6H, m, vinylic), 3.62 (3H, s, methyl ester), 2.96−2.84 (2H, m), 2.83−2.75 (2H, m), 2.44−2.15 (5H, m), 2.06−1.98 (3H, m), 1.65−1.56 (2H, m), 1.54−1.47 (2H, m), 1.40−1.21 (10H, m), and 0.86 (3H, t, J = 6.4 Hz, terminal aliphatic); ^{13}C NMR (100 MHz, $CDCl_3$) δ 173.98, 132.75, 132.34, 130.84, 130.71, 130.60, 130.46, 130.43, 130.36, 130.20, 130.03, 128.72, 128.59, 127.71, 127.56, 127.45, 127.39, 127.13, 124.47, 124.35, 124.17, 124.04, 124.01, 123.67, 57.05, 56.87, 56.39, 56.35, 56.26, 56.23, 51.33, 33.95, 33.85, 31.69, 31.47, 29.66, 29.27, 29.20, 29.13, 28.97, 28.73, 27.72, 27.59, 27.37, 27.19, 26.99, 26.32, 26.26, 26.19, 26.16, 25.77, 25.61, 24.79, 22.56, 22.53, and 14.00; HRESIMS m/z 385.2749 $[M + Na]^+$ (calcd for $C_{23}H_{38}NaO_3^+$, 385.2713). The ratio of 16,17-, 13,14-, 10,11-, and 7,8-EDT methyl ester regioisomers in the mixture was determined to be 2.0:1.7:1.7:1.0, respectively. The methyl ester form is frequently employed as a prodrug for EpFA application in both *in vitro* and *in vivo* disease models[25,34−37] and hence was utilized for pharmacological applications. The major advantages of the methyl esters are greater long-term stability and improved cell membrane permeability. They are rapidly cleaved to the biologically active carboxylic acid form by cellular esterases.[38,39] A time course for the formation of EDT free acids in HEK293 cells has been described in the Supporting Information (Figure S2).

Isolation of EDT Methyl Ester Regioisomers. The four EDT regioisomers were separated and isolated using a preparative chromatography system: Phenomenex Luna Silica 100 Å, LC 250 × 21.2 mm^2, 5 μm column in conjunction with a Waters 2489 UV/vis detector (monitoring at 200 nm), and a Waters Fraction Collector III. Preparative chromatography gradient conditions are given in the Supporting Information (Table S2).

Synthesis of DHDT Methyl Esters. This is shown with the representative 16,17-DHDT methyl ester. 5.8 mg (0.016 mmol) of 16,17-EDT methyl ester was dissolved in a solution of 0.5 mL of acetonitrile, 0.25 mL of H_2O, and 0.25 mL 8% perchloric acid and stirred overnight at room temperature. The mixture was directly purified by flash chromatography (ethyl acetate−hexanes 30:70).

Synthesis of EDT and DHDT Free Acids. This is shown with the representative 16,17-EDT free acid. To 30 μL of 30 mM 16,17-EDT methyl ester (in tetrahydrofuran (THF), 0.9 μmol, 1.00 equiv), 9 μL of 10 M NaOH (aq, 90 μmol, 100 equiv) was added. The reaction was stirred for 30 h at room temperature and quenched with 15 μL of acetic acid. The

https://dx.doi.org/10.1021/acsomega.1c00241
ACS Omega 2021, 6, 7165−7174

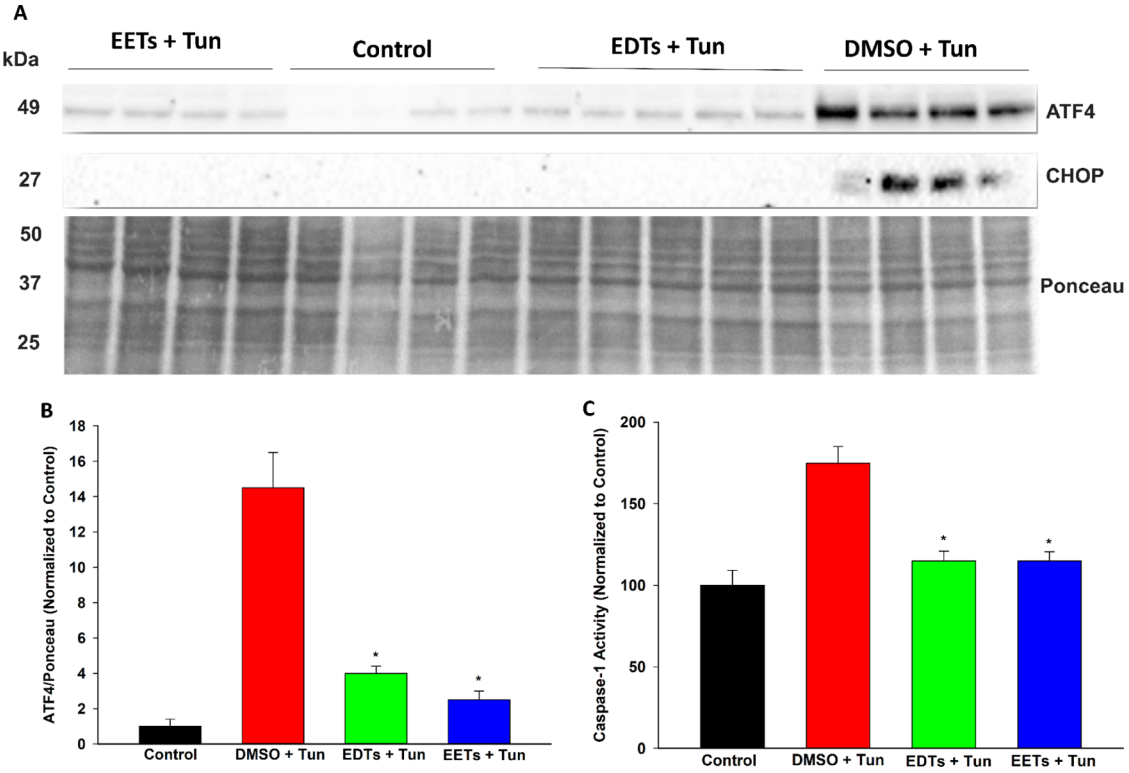

Figure 4. EDTs attenuate late-stage UPR markers and activity of an inflammatory caspase in tunicamycin (Tun)-triggered ER stress in HEK293 cells. (A) Immunoblots of ATF4 and CHOP for cells pretreated with EDTs (methyl esters, regioisomeric mixture, 1 μM), EETs, or DMSO for 1 h and exposed to 4 μg/mL Tun for 16 h. (B) EDTs (and EETs) significantly reduced ATF4 levels, relative to Ponceau loading control (one-way analysis of variance, Holm−Sidak method, *$p < 0.001$ *vs* DMSO + Tun group, $\alpha = 0.05$). (C) EDTs (and EETs) significantly decreased caspase-1 activity (one-way analysis of variance, Holm−Sidak method, *$p < 0.001$ *vs*. DMSO + Tun group, $\alpha = 0.05$).

mixture was directly purified by flash chromatography (ethyl acetate−hexanes−acetic acid 40:60:0.3). The ^{1}H NMR spectra and HRESIMS for the eight free acid analytes are described in the Supporting Information.

HPLC-MS/MS Method Optimization. The liquid chromatography system used for analysis was an Agilent 1200 SL liquid chromatography series (Agilent Technologies, Inc., Santa Clara, CA). The samples were placed in an autosampler and a volume of 5 μL was injected on a Kinetex C18 100 Å, LC 100 × 2.1 mm^2, 1.7 μm column, which was kept at 50 °C. Mobile Phase A was water with 0.1% glacial acetic acid, while Mobile Phase B was acetonitrile with 0.1% glacial acetic acid. A gradient elution (Table S3, Supporting Information) with a flow rate of 250 μL/min was employed and the chromatographic run was optimized to be 11 min for separation of analytes. The column was coupled to a 4000 Q-Trap tandem mass spectrometer (Applied Biosystems, Waltham, MA) equipped with an electrospray source (Turbo V), operating under a negative multiple reaction monitoring (MRM) mode. Mass spectrometer conditions are described in the Supporting Information (Table S4). Individual analyte standards were infused into the mass spectrometer to optimize source parameters (Table S5, Supporting Information) and identify unique MRM transitions. Source parameters and optimized MRM transitions of the internal standard CUDA, EETs, and DHETs are described in the Supporting Information (Table S6).

Calibration Curves and Linearity. All eight free acid analytes were dissolved in acetonitrile, and stock solutions were stored at −80 °C prior to use. Standard mixtures of eight different concentrations were prepared in 200 nM CUDA solution to determine calibration curves, linear ranges, and R^2 values *via* least-squares linear regression.

Solid-Phase Extraction. To obtain analytes from biological matrices for method validation and biological applications, solid-phase extraction was conducted, as previously described.[40] Oasis HLB 3cc Vac SPE Cartridges (60 mg Sorbent/Cartridge and 30 μm particle size), purchased from Waters Corp. (Milford, MA), were preconditioned, loaded with sample, washed, and dried. Analytes were then eluted, concentrated, and reconstituted in 200 nM CUDA.

Method Validation. The sensitivity, accuracy, precision, and recovery of the method were determined by analyzing quality control (QC) samples: human pooled plasma samples spiked with corresponding analytes. The limit of detection (LOD) and quantitation (LOQ) were estimated to be the minimum analyte concentration giving a signal-to-noise (S/N) ratio of >3 and >10, in a QC sample, respectively. Four replicates for each of four QC groups (unspiked, spiked at 1, 10, and 100 nM pre-extraction) were quantified within 24 h to estimate the intraday accuracy and precision. Interday accuracy and precision were assessed by analyzing samples over three different days. Similarly, analytical recovery was estimated by comparing recovered concentrations from QC samples spiked pre-extraction to QC samples spiked postextraction.

Biological Verification. All animal experiments were performed according to protocols approved by the Institutional Animal Care and Use Committee (IACUC) of University of California, Davis. For quantitation of basal EDT and DHDT levels, liver, kidney, brain, and plasma samples were collected

https://dx.doi.org/10.1021/acsomega.1c00241
ACS Omega 2021, 6, 7165−7174

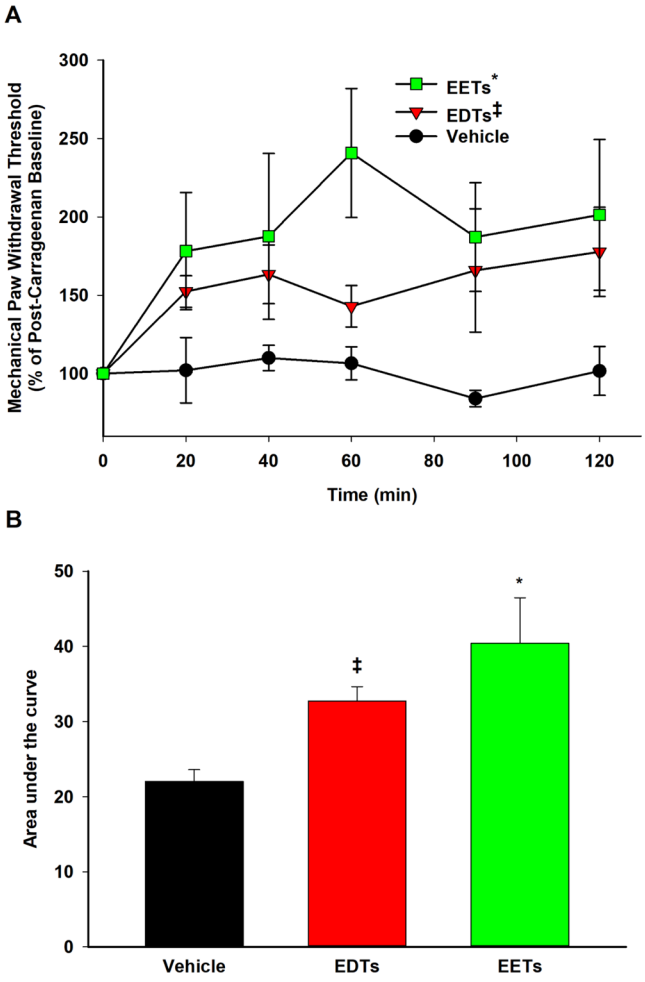

Figure 5. EDTs attenuate carrageenan-induced inflammatory pain in rats. (A) Following carrageenan (CARR, 0.5 mg/paw) administration, the painful post-CARR baseline was normalized to 100% and subsequent scores were calculated as the score × 100/CARR baseline. Thus, the increase in MWT scores (*i.e.*, above the painful CARR baseline) observed with EDTs (methyl esters, regioisomeric mixture, 300 ng/paw) treatment is indicative of antinociceptive effects. Scores are reported as the means ± standard error of the mean (SEM) of a group of rats per time point. Analgesic efficacy of EDTs (and EETs) was significant compared to the vehicle control (10% EtOH in saline) over a 2 h time course (two-way analysis of variance, Holm−Sidak method [factor: treatment], $^{*}p < 0.001$ *vs* vehicle, $^{\ddagger}p = 0.021$ *vs* vehicle, $\alpha = 0.05$). (B) Area under the curve (integrated from 0 to 120 min) represents the cumulative efficacy of a treatment and was significantly different for EDTs (and EETs) compared to the vehicle control (one-way analysis of variance, Holm−Sidak method, $^{*}p = 0.043$ *vs* vehicle, $^{\ddagger}p = 0.004$ *vs* vehicle, $\alpha = 0.05$).

from male Sprague−Dawley (SD) rats ($n = 6$), purchased from Charles River Laboratories. The animals were placed under deep isoflurane anesthesia, and blood was collected *via* cardiac puncture. The plasma fraction was separated through cold centrifugation at 4000 rpm for 10 min. Animals were euthanized with isoflurane and perfused with saline prior to tissue sampling. Tissue and plasma samples were flash-frozen and stored at −80 °C until metabolite extraction.

sEH Kinetics. To assess sEH-mediated hydrolysis of EDTs, a previously described enzyme kinetics assay was modified and applied.[25] A range of concentrations (0.04−5 mM) for each EDT methyl ester regioisomer were prepared in DMSO. One microliter of substrate solution was added to 90 μL of human carboxylesterase 2 ($[E]_{final}$ = 27 μg/mL) in sodium phosphate buffer (0.1 M, pH 7.4 w/freshly added 0.1 mg/mL bovine serum albumin (BSA)) and incubated overnight at 37 °C to facilitate complete conversion to the free acids. Ten microliters of purified, recombinant human sEH, in sodium phosphate buffer, was added ($[E]_{final}$ = 0.2 μg/mL), followed by incubation for 5−15 min at 37 °C. The reaction was quenched with 100 μL of 400 nM CUDA, and the amount of the corresponding DHDT formed was quantified *via* HPLC-MS/MS analysis. The rate of formation was plotted as a function of initial substrate concentration, and kinetic constants (K_M and V_{max}) were calculated *via* nonlinear regression using the enzyme kinetic module of SigmaPlot 14.0 (Systat Software, Inc., Chicago, IL). All measurements were performed in triplicates, and the mean is reported.

Cell Culture. Human embryonic kidney (HEK293) cells were purchased from American Type Culture Collection and cultured in Dulbecco's modified Eagle's medium supplemented with 10% fetal bovine serum and 1% penicillin−streptomycin. Cultures were maintained in a humidified incubator at 37 °C under an atmosphere of 5% CO_2/95% air.

3-(4,5-Dimethylthiazol-2-yl)-2,5-diphenyl Tetrazolium Bromide (MTT) Assay. HEK293 cells were seeded in poly-L-lysine-coated, clear-bottom black 96-well microplates at a density of approximately 1 × 10^4 cells/well and incubated overnight. Following pretreatment with EDT or EET methyl ester regioisomer mixtures (0.001−100 μM) for 1 h, cells were exposed to tunicamycin (4 μg/mL) for 24 h. The media was replaced with fresh media containing 0.5 mg/mL of the MTT reagent, and cells were incubated for 3 h at 37 °C. After the media was removed, the crystals were dissolved in 100% DMSO, and absorbance was read at 562 nm using a Tecan Infinite Pro microplate reader.

Caspase-1 Activity Assay. HEK293 cells were seeded in six-well plates at a density of approximately 3 × 10^5 cells/well and incubated overnight. Following pretreatment with EDT or EET methyl ester regioisomer mixtures (1 μM) for 1 h, cells were exposed to tunicamycin (4 μg/mL) for 16 h. An assay measuring caspase-1 activity was conducted as previously described.[41] Briefly, cells were rinsed with phosphate-buffered saline (PBS) and lysed with ice-cold radioimmunoprecipitation assay (RIPA) buffer. Following centrifugation, the supernatants were collected and stored on ice. Sixty microliters of supernatants were incubated with 60 μL of caspase activity buffer (containing 50 μM Ac-VAD-AFC, a fluorogenic caspase-1 substrate) for 2 h at 37 °C, after which fluorescence was read at $\lambda_{Ex}/\lambda_{Em}$ = 400/505 nm using a Molecular Device microplate reader.

Western Blotting. Confluent HEK293 cells in T75 flasks were pretreated with EDT or EET methyl ester regioisomer mixtures (1 μM) for 1 h, followed by tunicamycin (4 μg/mL) exposure for 5 or 16 h. Cells were rinsed with PBS, lysed with ice-cold RIPA buffer (containing freshly added protease and phosphatase inhibitors), homogenized, and centrifuged to collect supernatants. Protein concentrations in the lysates were estimated using a bicinchoninic acid (BCA) assay (Pierce). Proteins were denatured, separated by sodium dodecyl sulfate-polyacrylamide gel electrophoresis (SDS-PAGE), and transferred to nitrocellulose membranes. Membranes were stained with Ponceau stain and imaged using a charge-coupled device (CCD)-based digital imager for the protein loading control. Membranes were then blocked with 5% BSA or nonfat milk in

https://dx.doi.org/10.1021/acsomega.1c00241
ACS Omega 2021, 6, 7165−7174

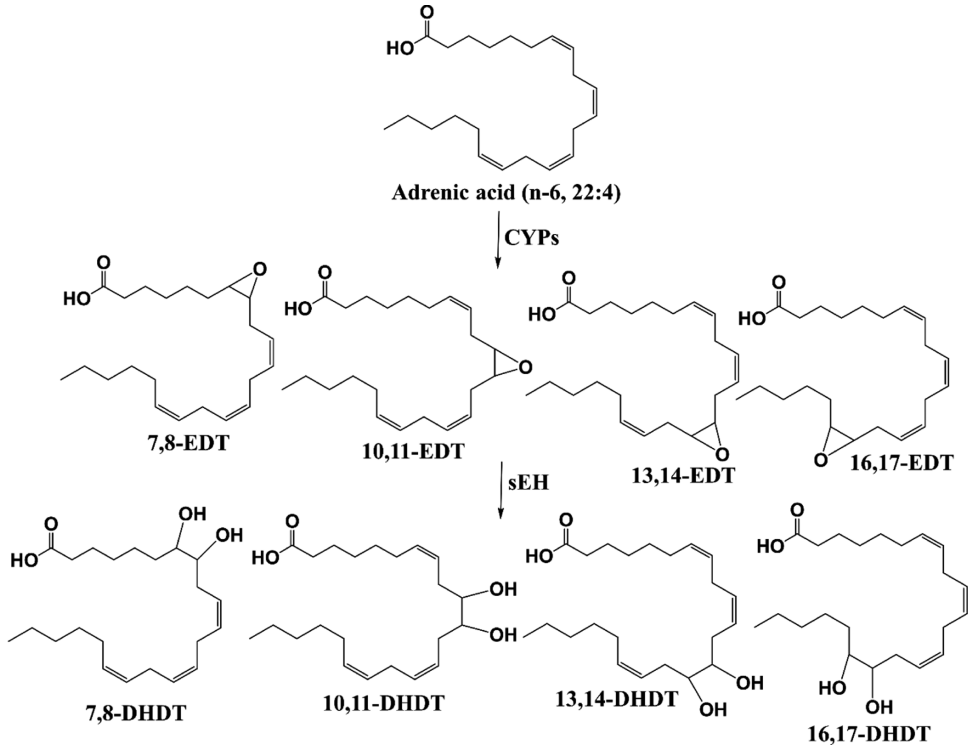

Figure 6. Cytochrome P450 (CYP) pathway of adrenic acid metabolism. Epoxydocosatrienoic acids (EDTs) are formed by CYP-mediated epoxidation of adrenic acid and are degraded downstream to dihydroxydocosatrienoic acids (DHDTs) by the soluble epoxide hydrolase (sEH).

tris-buffered saline with 0.05% Tween-20 for 1 h at room temperature, followed by incubation with the primary antibody (1:1000) overnight at 4 °C. Unbound antibody was washed off and membranes were incubated with a horseradish peroxidase (HRP)-conjugated secondary antibody (1:10 000) for 1 h at room temperature. Following washes, blots were exposed to an enhanced chemiluminescence (ECL) substrate (BioRad) under dark conditions for 2 min and bands were imaged.

Inflammatory Pain Model. A von Frey assay measuring mechanical withdrawal thresholds (MWT) was performed in male SD rats (n = 4−6/group), as previously described.[42] The study was conducted in a randomized and blinded manner. Prior to compound administration, rats were placed in clear, acrylic chambers and a baseline was assessed using an electronic von Frey aesthesiometer apparatus (IITC, Woodland Hills, CA). Carrageenan (CARR, 50 μL of a 1% solution, 0.5 mg) was then injected into the plantar area of the right hind paw. After three-and-a-half hours, post-CARR MWT were measured and normalized to 100%. Immediately after (t = 0), 10 μL of the vehicle control (10% EtOH in saline), EDT, or EET methyl ester regioisomer mixture (300 ng/paw) was administrated *via* intraplanar injection in the same paw. Ipsilateral MWT were assessed three to five times per rat per time point, over a 2 h time course (at 20, 40, 60, 90, and 120 min intervals), and scores were normalized relative to the post-CARR baseline.

■ ASSOCIATED CONTENT

Supporting Information

The Supporting Information is available free of charge at https://pubs.acs.org/doi/10.1021/acsomega.1c00241.

Intra and interday accuracy and precision and recovery of the developed analytical HPLC-MS/MS method; preparative HPLC gradient; analytical HPLC gradient; 4000 Q-Trap mass spectrometer conditions; MRM transitions for the internal standard, EETs, and DHETs; source parameters for all analytes; ^{1}H NMR and HRESIMS for EDT and DHDT regioisomers; and *in vitro* time course of EDT free acid formation (PDF)

■ AUTHOR INFORMATION

Corresponding Author

Bruce D. Hammock − *Department of Entomology and Nematology and UC Davis Comprehensive Cancer Center, University of California Davis, Davis, California 95616, United States;* orcid.org/0000-0003-1408-8317; Phone: 530-752-7519; Email: bdhammock@ucdavis.edu; Fax: 530-752-1537

Authors

Nalin Singh − *Department of Entomology and Nematology and UC Davis Comprehensive Cancer Center, University of California Davis, Davis, California 95616, United States;* orcid.org/0000-0002-6459-2987

Bogdan Barnych − *Department of Entomology and Nematology and UC Davis Comprehensive Cancer Center, University of California Davis, Davis, California 95616, United States*

Karen M. Wagner − *Department of Entomology and Nematology and UC Davis Comprehensive Cancer Center, University of California Davis, Davis, California 95616, United States*

Debin Wan − *Department of Entomology and Nematology and UC Davis Comprehensive Cancer Center, University of California Davis, Davis, California 95616, United States*

Christophe Morisseau − *Department of Entomology and Nematology and UC Davis Comprehensive Cancer Center,*

https://dx.doi.org/10.1021/acsomega.1c00241
ACS Omega 2021, 6, 7165−7174

University of California Davis, Davis, California 95616, United States

Complete contact information is available at: https://pubs.acs.org/10.1021/acsomega.1c00241

Notes

The authors declare no competing financial interest.

■ ACKNOWLEDGMENTS

This work was partially funded by National Institutes of Health grants, National Institute of Environmental Health Sciences (NIEHS) RIVER Award (R35 ES030443-01), NIEHS/Superfund Research Program (P42 ES004699), and National Institute of Diabetes and Digestive and Kidney Diseases (R01DK103616 and R01DK107767). N.S. thanks the NIEHS/UC Davis Superfund Research Program for financial support in the form of GSR fellowships.

■ REFERENCES

(1) Fisslthaler, B.; Popp, R.; Kiss, L.; Potente, M.; Harder, D. R.; Fleming, I.; Busse, R. Cytochrome P450 2C is an EDHF synthase in coronary arteries. *Nature* **1999**, *401*, 493−497.

(2) Imig, J. D.; Zhao, X.; Capdevila, J. H.; Morisseau, C.; Hammock, B. D. Soluble epoxide hydrolase inhibition lowers arterial blood pressure in angiotensin II hypertension. *Hypertension* **2002**, *39*, 690−694.

(3) Inceoglu, B.; Jinks, S. L.; Ulu, A.; Hegedus, C. M.; Georgi, K.; Schmelzer, K. R.; Wagner, K.; Jones, P. D.; Morisseau, C.; Hammock, B. D. Soluble epoxide hydrolase and epoxyeicosatrienoic acids modulate two distinct analgesic pathways. *Proc. Natl. Acad. Sci. U.S.A.* **2008**, *105*, 18901−18906.

(4) Liu, L.; Chen, C.; Gong, W.; Li, Y.; Edin, M. L.; Zeldin, D. C.; Wang, D. W. Epoxyeicosatrienoic acids attenuate reactive oxygen species level, mitochondrial dysfunction, caspase activation, and apoptosis in carcinoma cells treated with arsenic trioxide. *J. Pharmcol. Exp. Ther.* **2011**, *339*, 451−463.

(5) Xu, X.; Tu, L.; Feng, W.; Ma, B.; Li, R.; Zheng, C.; Li, G.; Wang, D. W. CYP2J3 gene delivery up-regulated adiponectin expression via reduced endoplasmic reticulum stress in adipocytes. *Endocrinology* **2013**, *154*, 1743−1753.

(6) Rosenthal, M. D.; Hill, J. R. Elongation of arachidonic and eicosapentaenoic acids limits their availability for thrombin-stimulated release from the glycerolipids of vascular endothelial cells. *Biochim. Biophys. Acta, Lipids Lipid Metab.* **1986**, *875*, 382−391.

(7) Mann, C. J.; Kaduce, T. L.; Figard, P. H.; Spector, A. A. Docosatetraenoic acid in endothelial cells: formation, retroconversion to arachidonic acid, and effect on prostacyclin production. *Arch. Biochem. Biophys.* **1986**, *244*, 813−823.

(8) Rosenthal, M. D.; Hill, J. R. Human vascular endothelial cells synthesize and release 24- and 26-carbon polyunsaturated fatty acids. *Biochim. Biophys. Acta, Lipids Lipid Metab.* **1984**, *795*, 171−178.

(9) Mimouni, V.; Narce, M.; Huang, Y. S.; Horrobin, D. F.; Poisson, J. P. Adrenic acid Δ4 desaturation and fatty acid composition in liver microsomes of spontaneously diabetic Wistar BB rats. *Prostaglandins, Leukotrienes Essent. Fatty Acids* **1994**, *50*, 43−47.

(10) Wijendran, V.; Lawrence, P.; Diau, G. Y.; Boehm, G.; Nathanielsz, P. W.; Brenna, J. T. Significant utilization of dietary arachidonic acid is for brain adrenic acid in baboon neonates. *J. Lipid Res.* **2002**, *43*, 762−767.

(11) Sprecher, H.; VanRollins, M.; Sun, F.; Wyche, A.; Needleman, P. Dihomo-prostaglandins and -thromboxane. A prostaglandin family from adrenic acid that may be preferentially synthesized in the kidney. *J. Biol. Chem.* **1982**, *257*, 3912−3918.

(12) Yi, X.-Y.; Gauthier, K. M.; Cui, L.; Nithipatikom, K.; Falck, J. R.; Campbell, W. B. Metabolism of adrenic acid to vasodilatory 1alpha,1beta-dihomo-epoxyeicosatrienoic acids by bovine coronary arteries. *Am. J. Physiol.: Heart Circ. Physiol.* **2007**, *292*, H2265−H2274.

(13) Kopf, P. G.; Zhang, D. X.; Gauthier, K. M.; Nithipatikom, K.; Yi, X. Y.; Falck, J. R.; Campbell, W. B. Adrenic acid metabolites as endogenous endothelium-derived and zona glomerulosa-derived hyperpolarizing factors. *Hypertension* **2010**, *55*, 547−554.

(14) Zhang, Y.; Oltman, C. L.; Lu, T.; Lee, H.-C.; Dellsperger, K. C.; VanRollins, M. EET homologs potently dilate coronary microvessels and activate BK(Ca) channels. *Am. J. Physiol.: Heart Circ. Physiol.* **2001**, *280*, H2430−H2440.

(15) Gebremedhin, D.; Ma, Y. H.; Falck, J. R.; Roman, R. J.; VanRollins, M.; Harder, D. R. Mechanism of action of cerebral epoxyeicosatrienoic acids on cerebral arterial smooth muscle. *Am. J. Physiol.: Heart Circ. Physiol.* **1992**, *263*, H519−H525.

(16) Campbell, W. B.; Gebremedhin, D.; Pratt, P. F.; Harder, D. R. Identification of epoxyeicosatrienoic acids as endothelium-derived hyperpolarizing factors. *Circ. Res.* **1996**, *78*, 415−423.

(17) Archer, S. L.; Gragasin, F. S.; Wu, X.; Wang, S.; McMurtry, S.; Kim, D. H.; Platonov, M.; Koshal, A.; Hashimoto, K.; Campbell, W. B.; Falck, J. R.; Michelakis, E. D. Endothelium-derived hyperpolarizing factor in human internal mammary artery is 11,12-epoxyeicosatrienoic acid and causes relaxation by activating smooth muscle BK(Ca) channels. *Circulation* **2003**, *107*, 769−776.

(18) Sadler, N. C.; Nandhikonda, P.; Webb-Robertson, B.-J.; Ansong, C.; Anderson, L. N.; Smith, J. N.; Corley, R. A.; Wright, A. T. Hepatic Cytochrome P450 Activity, Abundance, and Expression Throughout Human Development. *Drug Metab. Dispos.* **2016**, *44*, 984−991.

(19) Gill, S. S.; Hammock, B. D. Distribution and properties of a mammalian soluble epoxide hydrase. *Biochem. Pharmacol.* **1980**, *29*, 389−395.

(20) Håkansson, I.; Gouveia-Figueira, S.; Ernerudh, J.; Vrethem, M.; Ghafouri, N.; Ghafouri, B.; Nording, M. Oxylipins in cerebrospinal fluid in clinically isolated syndrome and relapsing remitting multiple sclerosis. *Prostaglandins Other Lipid Mediators* **2018**, *138*, 41−47.

(21) Lucas, D.; Goulitquer, S.; Marienhagen, J.; Fer, M.; Dreano, Y.; Schwaneberg, U.; Amet, Y.; Corcos, L. Stereoselective epoxidation of the last double bond of polyunsaturated fatty acids by human cytochromes P450. *J. Lipid Res.* **2010**, *51*, 1125−1133.

(22) McDougle, D. R.; Watson, J. E.; Abdeen, A. A.; Adili, R.; Caputo, M. P.; Krapf, J. E.; Johnson, R. W.; Kilian, K. A.; Holinstat, M.; Das, A. Anti-inflammatory ω-3 endocannabinoid epoxides. *Proc. Natl. Acad. Sci. U.S.A.* **2017**, *114*, E6034−E6043.

(23) Singh, N.; Hammock, B. D. Soluble Epoxide Hydrolase. In *Encyclopedia of Molecular Pharmacology*; 3rd ed.; Offermanns, S.; Rosenthal, W., Eds.; Springer International Publishing, Cham, 2020; pp 1−7.

(24) Morisseau, C.; Wecksler, A. T.; Deng, C.; Dong, H.; Yang, J.; Lee, K. S.; Kodani, S. D.; Hammock, B. D. Effect of soluble epoxide hydrolase polymorphism on substrate and inhibitor selectivity and dimer formation. *J. Lipid Res.* **2014**, *55*, 1131−1138.

(25) Morisseau, C.; Inceoglu, B.; Schmelzer, K.; Tsai, H. J.; Jinks, S. L.; Hegedus, C. M.; Hammock, B. D. Naturally occurring monoepoxides of eicosapentaenoic acid and docosahexaenoic acid are bioactive antihyperalgesic lipids. *J. Lipid Res.* **2010**, *51*, 3481−3490.

(26) Argiriadi, M. A.; Morisseau, C.; Goodrow, M. H.; Dowdy, D. L.; Hammock, B. D.; Christianson, D. W. Binding of alkylurea inhibitors to epoxide hydrolase implicates active site tyrosines in substrate activation. *J. Biol. Chem.* **2000**, *275*, 15265−15270.

(27) Sano, R.; Reed, J. C. ER stress-induced cell death mechanisms. *Biochim. Biophys. Acta, Mol. Cell Res.* **2013**, *1833*, 3460−3470.

(28) Inceoglu, B.; Bettaieb, A.; Haj, F. G.; Gomes, A. V.; Hammock, B. D. Modulation of mitochondrial dysfunction and endoplasmic reticulum stress are key mechanisms for the wide-ranging actions of epoxy fatty acids and soluble epoxide hydrolase inhibitors. *Prostaglandins Other Lipid Mediators* **2017**, *133*, 68−78.

(29) Abdullahi, A.; Stanojcic, M.; Parousis, A.; Patsouris, D.; Jeschke, M. G. Modeling Acute ER Stress in Vivo and in Vitro. *Shock* **2017**, *47*, 506−513.
(30) Lebeaupin, C.; Proics, E.; de Bieville, C. H.; Rousseau, D.; Bonnafous, S.; Patouraux, S.; Adam, G.; Lavallard, V. J.; Rovere, C.; Le Thuc, O.; Saint-Paul, M. C.; Anty, R.; Schneck, A. S.; Iannelli, A.; Gugenheim, J.; Tran, A.; Gual, P.; Bailly-Maitre, B. ER stress induces NLRP3 inflammasome activation and hepatocyte death. *Cell Death Dis.* **2015**, *6*, No. e1879.
(31) Inceoglu, B.; Schmelzer, K. R.; Morisseau, C.; Jinks, S. L.; Hammock, B. D. Soluble epoxide hydrolase inhibition reveals novel biological functions of epoxyeicosatrienoic acids (EETs). *Prostaglandins Other Lipid Mediators* **2007**, *82*, 42−49.
(32) Liu, J.-Y. Inhibition of Soluble Epoxide Hydrolase for Renal Health. *Front. Pharmacol.* **2019**, *9*, No. 1551.
(33) Hashimoto, K. Role of Soluble Epoxide Hydrolase in Metabolism of PUFAs in Psychiatric and Neurological Disorders. *Front. Pharmacol.* **2019**, *10*, No. 36.
(34) Abdu, E.; Bruun, D. A.; Yang, D.; Yang, J.; Inceoglu, B.; Hammock, B. D.; Alkayed, N. J.; Lein, P. J. Epoxyeicosatrienoic acids enhance axonal growth in primary sensory and cortical neuronal cell cultures. *J. Neurochem.* **2011**, *117*, 632−642.
(35) Inceoglu, B.; Zolkowska, D.; Yoo, H. J.; Wagner, K. M.; Yang, J.; Hackett, E.; Hwang, S. H.; Lee, K. S. S.; Rogawski, M. A.; Morisseau, C.; Hammock, B. D. Epoxy Fatty Acids and Inhibition of the Soluble Epoxide Hydrolase Selectively Modulate GABA Mediated Neurotransmission to Delay Onset of Seizures. *PLoS One* **2013**, *8*, No. e80922.
(36) Supp, D. M.; Hahn, J. M.; McFarland, K. L.; Combs, K. A.; Lee, K. S. S.; Inceoglu, B.; Wan, D.; Boyce, S. T.; Hammock, B. D. Soluble Epoxide Hydrolase Inhibition and Epoxyeicosatrienoic Acid Treatment Improve Vascularization of Engineered Skin Substitutes. *Plast. Reconstr. Surg. Global Open* **2016**, *4*, No. e1151.
(37) Wagner, K.; Lee, K. S.; Yang, J.; Hammock, B. D. Epoxy fatty acids mediate analgesia in murine diabetic neuropathy. *Eur. J. Pain* **2017**, *21*, 456−465.
(38) Greene, J. F.; Williamson, K. C.; Newman, J. W.; Morisseau, C.; Hammock, B. D. Metabolism of monoepoxides of methyl linoleate: bioactivation and detoxification. *Arch. Biochem. Biophys.* **2000**, *376*, 420−432.
(39) Greene, J. F.; Newman, J. W.; Williamson, K. C.; Hammock, B. D. Toxicity of epoxy fatty acids and related compounds to cells expressing human soluble epoxide hydrolase. *Chem. Res. Toxicol.* **2000**, *13*, 217−226.
(40) Yang, J.; Schmelzer, K.; Georgi, K.; Hammock, B. D. Quantitative Profiling Method for Oxylipin Metabolome by Liquid Chromatography Electrospray Ionization Tandem Mass Spectrometry. *Anal. Chem.* **2009**, *81*, 8085−8093.
(41) Furuoka, M.; Ozaki, K.; Sadatomi, D.; Mamiya, S.; Yonezawa, T.; Tanimura, S.; Takeda, K. TNF-α Induces Caspase-1 Activation Independently of Simultaneously Induced NLRP3 in 3T3-L1 Cells. *J. Cell. Physiol.* **2016**, *231*, 2761−2767.
(42) Wagner, K.; Inceoglu, B.; Dong, H.; Yang, J.; Hwang, S. H.; Jones, P.; Morisseau, C.; Hammock, B. D. Comparative efficacy of 3 soluble epoxide hydrolase inhibitors in rat neuropathic and inflammatory pain models. *Eur. J. Pharmacol.* **2013**, *700*, 93−101.

https://dx.doi.org/10.1021/acsomega.1c00241
ACS Omega 2021, 6, 7165−7174